

## Redox Conduction in Electropolymerized Films of Transition-Metal Complexes of Os, Ru, Fe, and Co

Helen C. Hurrell and Héctor D. Abruña\*

Received July 14, 1989

Conductances were measured for mixed-valent electropolymerized films of transition-metal complexes of the type  $[M(v\text{-bpy})_x(L)_m]$  ( $M = \text{Os, Ru, Fe, Co}$ ;  $v\text{-bpy} = 4\text{-vinyl-4'-methyl-2,2'-bipyridine}$ ;  $L = \text{cyano, phenanthroline derivatives}$ ). Trends in conductance were attributed to the size of the metal center, back-bonding ability of the ligands, and the distance between localized states. The mechanism of the charge transport was investigated by examining the effects of temperature, solvent, and electrolyte on the conductances. The results suggest two possible mechanisms of charge propagation dependent on electron motion from either metal- or ligand-localized orbitals. Solvent effects paralleled outer-sphere electron transfer in solution as described by the Marcus theory.

### Introduction

Electron mobility in electroactive polymer films is essential for electrocatalytic,<sup>1</sup> electronic device,<sup>2</sup> and photoelectrochemical<sup>3</sup> applications. Electron transport in polymer films of metal-centered electropolymerizable complexes is thought to proceed via electron hopping between discrete localized valence states, resembling a diffusion process dependent on the mixed-valent nature of the film.<sup>4</sup> In this mixed-valent state, the highest occupied valence shell is only partially filled. The driving force for the redox conduction at room temperature arises from the concentration gradients of redox sites across the film, whereas at lower temperatures, when the counteranion becomes immobile, voltage gradients can become important.<sup>5</sup>

In contrast, electronically conducting polymer films, which are ohmic in nature, respond to an applied electric potential manifested as an electrostatic potential gradient. Electronic conduction has been observed in valence-localized polymers when counterions have been excluded from the film during changes in polymer oxidation state, thus driving electron hopping by electrical potential gradients.<sup>6</sup> Such electronic conduction requires partially unoccupied low-energy delocalized electronic states for the electron mobility.

Polymers exhibiting redox or electronic conductivity have been examined. Linear-chain polyorganics such as polyaniline and polypyrrole have been prepared with electronic conductivities as high as 0.1 S/cm.<sup>7</sup> Stacked phthalocyanines<sup>8</sup> and poly(sulfur nitride)  $((\text{SN})_x)$ <sup>9</sup> have been shown to act as electronic conductors. Redox-conducting polymers such as poly- $[\text{Ru}(v\text{-bpy})_3]^{2+}$  ( $v\text{-bpy} = 4\text{-vinyl-4'-methyl-2,2'-bipyridine}$ ) have been demonstrated to reach conductivities of  $1 \times 10^{-5}$  S/cm,<sup>10</sup> a value that lies in the range of some semiconductors.

The redox conduction of osmium polypyridine polymers has been measured with polymer films sandwiched between two

electrodes in which one is porous to the flow of solvent and electrolyte. The spacing between the electrodes is small (approximately 1000 Å), thus allowing concentration gradients of oxidation state to be maintained across the polymer film. Steady-state currents are established, and from these the charge-transfer diffusion coefficients can be obtained. Maximum redox conduction was obtained when the film contained equal quantities of Os(III) and Os(II) states, since this condition gives rise to the highest concentration gradients through the film.<sup>11</sup> Further studies of osmium polypyridine films demonstrated the importance of the mixed-valent state Os(I/0) for the generation of redox conduction currents.<sup>12</sup>

In the present study, a wide range of redox-conducting polymers of the type poly- $[\text{M}(v\text{-bpy})_x(L)_y]$  ( $M = \text{Co, Fe, Ru, Os}$ ;  $L = v\text{-bpy, phen-dione (phenanthroline-5,6-dione), 4-Me-phen, 5-NH}_2\text{-phen, 5-Cl-phen, cyano}$ ) have been investigated to elucidate the effects of the metal center, the electronic contribution of the ligands, and the oxidation state of the complex on the conductivity. The complexes are of similar size, with six nitrogens in octahedral coordination around the metal center, and are electropolymerized into thick (approximately 1000 equivalent monolayers), amorphous films. Thus, solvent swelling abilities and the size of the charge-trapping unit can be maintained relatively constant, a factor that is essential since both of these effects are known to greatly affect electron transport and thus conductivity.

### Experimental Section

**1. Electrodes.** Platinum-array electrodes consisting of three parallel platinum lengths separated by insulating material of 5–10  $\mu\text{m}$  were constructed as previously described.<sup>13</sup> Briefly, three parallel platinum sheets (approximately 2 mm in length and 20  $\mu\text{m}$  thick) were sandwiched between glass slides and separated by thin sheets of mylar (approximately 5  $\mu\text{m}$  thick). The assembly was sealed together with epoxy glue (Epon 828 and 14% *m*-phenylenediamine) so that only the cross sections of the parallel platinum sheets were exposed. Prior to the use, the electrodes were polished with diamond paste (Buehler) and thoroughly rinsed with water and acetone.

**2. Reagents.** Acetonitrile ( $\text{CH}_3\text{CN}$ ), *N,N'*-dimethylformamide (DMF), methylene chloride ( $\text{CH}_2\text{Cl}_2$ ), and dimethyl sulfoxide (DMSO) (all Burdick and Jackson, distilled in glass) were dried over 4-Å molecular sieves prior to use. Tetra-*n*-butylammonium perchlorate (TBAP, G. F. Smith) and tetra-*n*-butylammonium tetrafluoroborate ( $(\text{TBA})\text{BF}_4$ , G. F. Smith) were recrystallized three times from ethyl acetate and dried under vacuum at 70 °C for 72 h.

Tetra-*n*-butylammonium hexafluorophosphate ( $(\text{TBA})\text{PF}_6$ ) was prepared by mixing equimolar quantities of tetra-*n*-butylammonium bromide and ammonium hexafluorophosphate in acetone. Solid ammonium bromide was filtered off, and the eluent was added to 5% aqueous potassium hexafluorophosphate. The crude product was precipitated and redissolved in acetone, the solution refiltered, and the solid reprecipitated in 5% aqueous potassium hexafluorophosphate. The product was collected, washed with water, recrystallized twice from 50% ethanol/50% water, and vacuum dried at 80 °C for 48 h.

Tetramethylammonium *p*-toluenesulfonate ( $(\text{TMA})\text{Ts}$ ) was prepared by mixing equimolar quantities of tetramethylammonium hydroxide

- (1) (a) Murray, R. W. *Electroanal. Chem.* **1984**, *13*, 191. (b) Abruña, H. D. *Coord. Chem. Rev.* **1988**, *86*, 135.
- (2) (a) Pickup, P. G.; Murray, R. W. *J. Electrochem. Soc.* **1984**, *131*, 833. (b) Kittleson, G. P.; White, H. S.; Wrighton, M. S. *J. Am. Chem. Soc.* **1984**, *106*, 7389. (c) Wrighton, M. S. *Science* **1986**, *231*, 32. (d) Chidsey, C. E. D.; Murray, R. W. *Science* **1986**, *231*, 25.
- (3) Bard, A. J. *J. Chem. Educ.* **1983**, *60*, 302.
- (4) Kaufman, F. B.; Schroeder, A. H.; Engler, E. M.; Kramer, S. R.; Chambers, J. Q. *J. Am. Chem. Soc.* **1980**, *102*, 483.
- (5) Jernigan, J. C.; Murray, R. W. *J. Phys. Chem.* **1987**, *91*, 2030.
- (6) (a) Elliott, C. M.; Redepenning, J. G.; Schmitt, S. J.; Balk, E. M. In *Inorganic and Organometallic Polymers*; Zeldin, M., Wynne, K., Allcock, H. R., Eds.; American Chemical Society: Washington, DC, 1988; p 430. (b) Elliott, C. M.; Redepenning, J. C.; Balk, E. M. *J. Electroanal. Chem. Interfacial Electrochem.* **1986**, *213*, 203. (c) Elliott, C. M.; Redepenning, J. G.; Balk, E. M. *J. Am. Chem. Soc.* **1985**, *107*, 8302.
- (7) (a) Pfluger, P.; Krounbi, M.; Street, G. B.; Weiser, G. J. *J. Chem. Phys.* **1983**, *78*, 3212. (b) Feldman, B. J.; Burgmayer, P.; Murray, R. W. *J. Am. Chem. Soc.* **1985**, *107*, 872.
- (8) (a) Marks, T. J. *Science* **1985**, *227*, 881. (b) Petersen, J. L.; Schramm, C. S.; Stojakovic, D. R.; Hoffman, B. M.; Marks, T. J. *J. Am. Chem. Soc.* **1977**, *99*, 286. (c) Hoffman, B. M.; Ibers, J. A. *Acc. Chem. Res.* **1983**, *16*, 15. (d) Hanack, M. *Mol. Cryst. Liq. Cryst.* **1984**, *105*, 133.
- (9) Walatka, V. V.; Labes, M. M.; Perlstein, J. H. *Phys. Rev. Lett.* **1973**, *31*, 1139.
- (10) (a) Chidsey, C. E. D.; Murray, R. W. *J. Phys. Chem.* **1986**, *90*, 1479. (b) Chidsey, C. E. D.; Feldman, B. J.; Lundgren, C.; Murray, R. W. *Anal. Chem.* **1986**, *58*, 601.

- (11) Pickup, P. G.; Murray, R. W. *J. Am. Chem. Soc.* **1983**, *105*, 4510.
- (12) Pickup, P. G.; Kutner, W.; Leidner, C. R.; Murray, R. W. *J. Am. Chem. Soc.* **1984**, *106*, 1991.
- (13) Hurrell, H. C.; Abruña, H. D. *Mol. Cryst. Liq. Cryst.* **1988**, *160*, 377.

(20% in methanol) and aqueous *p*-toluenesulfonic acid. The solution was stirred for 1 h, at which time the methanol was removed by rotary evaporation. The precipitate was collected, recrystallized twice from acetonitrile, and vacuum dried at 70 °C for 48 h.

Poly(vinyl acetate) (PVA, Aldrich) with an average molecular weight of 113 000 Do. was dissolved in acetonitrile to vary the solvent viscosity. Viscosities were measured with a Canon-Ubbelohde viscometer.

Synthesis and electropolymerization of  $[\text{Fe}(\text{v-bpy})_3]^{2+}$ ,  $[\text{Os}(\text{v-bpy})_3]^{2+}$ ,  $[\text{Ru}(\text{v-bpy})_3]^{2+}$ , and  $[\text{Fe}(\text{v-bpy})_2(\text{CN})_2]^{2+}$  have been described elsewhere.<sup>14</sup>  $[\text{Co}(\text{v-terpy})_2]^{2+}$  (v-terpy = 4'-vinyl-2,2':6',2''-terpyridine) was prepared as previously described.<sup>15</sup>

$[\text{Os}(\text{v-bpy})_2(5\text{-NH}_2\text{-phen})]^{2+}$ ,  $[\text{Os}(\text{v-bpy})_2(\text{phen-dione})]^{2+}$ , and  $[\text{Os}(\text{v-bpy})_2(4\text{-Me-phen})]^{2+}$  were prepared by dissolving  $[\text{Os}(\text{v-bpy})_2\text{Cl}_2]$ , prepared as described,<sup>15</sup> in ethylene glycol with a 3-fold molar excess of the phenanthroline ligand. The solution was refluxed under nitrogen for 3 h, at which time an equal volume of water was added to the cooled reaction mixture. The complexes were precipitated with  $\text{KPF}_6$ . The collected precipitate was purified by passage through a neutral alumina column using acetonitrile as the eluant. Due to the strong adsorption of the  $[\text{Os}(\text{v-bpy})_2(\text{phen-dione})]^{2+}$  complex to alumina, it was purified by dissolution in acetonitrile and reprecipitation in diethyl ether.

$[\text{Os}(5\text{-Cl-phen})_3]^{2+}$  (5-Cl-phen = 5-chloro-1,10-phenanthroline) was prepared by dissolving  $(\text{NH}_4)_2\text{OsCl}_6$  in ethylene glycol with a 6-fold molar excess of 5-Cl-phen. The solution was refluxed under nitrogen for 12 h, and the complex was precipitated by the addition of saturated aqueous  $\text{NH}_4\text{PF}_6$ . The complex was purified by passage through a neutral alumina column eluted with 1:1 acetonitrile/toluene, as previously described.<sup>16</sup>

Electropolymerization of the monomer complexes was achieved as previously described.<sup>14,18</sup> For example, thick polymer films of  $[\text{Os}(\text{v-bpy})_2(\text{phen-dione})]^{2+}$  can be prepared by shorting the three electrodes of the array together and scanning the potential continuously from 0.0 to  $-1.80$  V vs SSCE in a 1 mM  $\text{CH}_3\text{CN}/0.1$  M TBAP solution of the complex. Surface coverages ( $\Gamma$ ) were determined by measuring the charge under the cyclic voltammetric peak obtained at slow scan rate (10 mV/s) and corresponding to the metal(II/III) oxidation. Polymer coverages of  $(1-9) \times 10^{-8}$  mol/cm<sup>2</sup> were used in the conductivity experiments as these coverages were sufficient to bridge the insulating gap between the electrodes of the array.

**3. Instrumentation.** Electrochemical experiments were performed on a Pine Instruments RD-4 bipotentiostat, and data were recorded on a Soltec X-Y-Y recorder. A conventional electrochemical cell was employed with a platinum counter electrode and a saturated sodium calomel reference electrode (SSCE). All potentials are referenced to this electrode without regard for the liquid junction. All experiments were carried out in a Faraday cage to minimize noise.

Temperature-controlled experiments were performed by using an Omega temperature controller with two hotwatt resistive heaters inside a copper block configured as described previously.<sup>13</sup>

**4. Conductance Measurements.** Conductance measurements were made in a fresh  $\text{CH}_3\text{CN}/0.1$  M TBAP solution after the modified electrodes had been rinsed with acetone and dried. The polymer-coated array was left in the  $\text{CH}_3\text{CN}$  solution for 10 min prior to the measurement to allow for swelling of the polymer film. The conductance between two noncontiguous electrodes mediated by the polymer film was measured while the potential applied to the center electrode was varied with respect to a reference electrode in solution, thus changing the oxidation state of the polymer film. Both current (i.e. cyclic voltammogram) and conductance were recorded simultaneously. Several repetitions of the cyclic voltammogram confirmed that the films were stable and that there was no loss of polymer material between successive scans.

Conductance through the polymer films was measured as either a voltage drop between the two outer electrodes or as a voltage across a 50-M $\Omega$  high-precision Victoreen resistor with a variable load (0–200

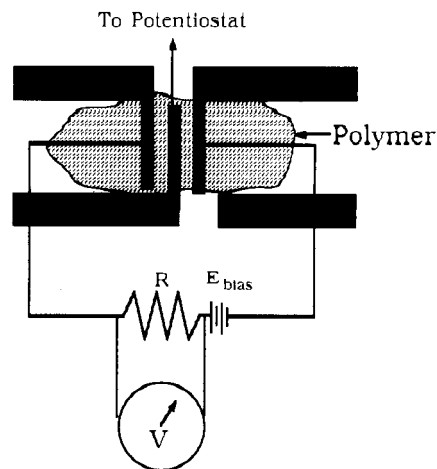


**Figure 1.** Schematic diagram for the conductance-measuring circuit for the array electrodes.

mV), as illustrated in Figure 1. Conductance values were converted to conductivities after measuring the film dimensions.

In order to determine how film thickness varied as a function of the polymer coverage, we employed electropolymerized films of  $[\text{Os}(\text{v-bpy})_3]^{2+}$  on platinum sputtered onto glass slides. The complex was electropolymerized onto the large area electrode surface and rinsed with  $\text{CH}_3\text{CN}$ . Immediately following the rinse, the swollen polymer film thickness was measured with a Sloan profilometer. Although the time between emersion and measurement was typically very short, there is some uncertainty in the thickness measurements since the emersed polymer films were measured.

## Results and Discussion

The electrochemical polymerization technique for the complexes utilized in this study relied on radical-induced polymerization involving the reduced form of vinylbipyridine.<sup>18</sup> Linkages between complexes consisted of four C–C bond lengths. When phenanthroline derivatives were substituted for one of the v-bpy ligands, the coupling reaction was similar, with coupling of the vinyl moiety usually taking place at the 4- or 7-position on the phenanthroline.<sup>19</sup> The (5-Cl-phen)<sub>3</sub> complex could be reductively polymerized with concomitant loss of chloride. In this case the polymer formed an organic backbone similar to the complexes described above with a single C–C bond length spacing between the monomer units.<sup>16</sup> In all cases, the polymer films were stable to repeated electrochemical cycling, highly reproducible, well-behaved, and generated linear  $i_p$  versus  $v^{1/2}$  plots. In most cases, thick films consisting of at least 1000 equivalent monomers could be deposited.

The polymer films were examined by light microscopy, which showed that the films extended to about 20  $\mu\text{m}$  beyond the electrode region. We were thus confident that the polymer extended not only across the electrode regions but also across the insulating gaps.

Conductance measurements across polymer films under potentiostatic control include the superposition of a number of contributions.

First, the potential applied to the center electrode (via the potentiostat) generates gradients in the concentration of redox species that migrate in a transverse fashion toward the outer two electrodes. The movement of charge through the polymer associated with these concentration gradients depends on the exact distance to be traversed, the local film thickness, and the redox conductivity of the film. Thus, when a potential was applied to the center electrode (notwithstanding the value of the applied bias potential or the load resistance), a potential drop, dependent upon the conductivity of the film, could be measured across the outer two electrodes. Although reproducibly systematic trends could be measured (allowing for relative comparisons to be made) absolute conductances could not be measured.

Another contribution to the conductivity measurement was that observed in response to the external circuit. The potential mea-

- (14) (a) Denisevich, P.; Abruña, H. D.; Leidner, C. R.; Meyer, T. J.; Murray, R. W. *Inorg. Chem.* **1982**, *21*, 2153. (b) Bryant, G. M.; Fergusson, J. E.; Powell, H. K. *J. Aust. J. Chem.* **1971**, *24*, 257. (c) Schilt, A. A. *J. Am. Chem. Soc.* **1960**, *82*, 3000. (d) Martin, V.; Nyholm, R. S. *J. Chem. Soc.* **1958**, 4284. (e) Dwyer, F. P. *J. Proc. R. Soc.* **1949**, *83*, 134. (f) Buckingham, D. A.; Dwyer, F. P.; Goodwin, H. A.; Sargeson, A. M. *Aust. J. Chem.* **1964**, *17*, 325. (g) Braddock, J. N.; Meyer, T. J. *J. Am. Chem. Soc.* **1973**, *95*, 3185.
- (15) Kokber, E. M.; Caspar, J. V.; Sullivan, B. P.; Meyer, T. J. *Inorg. Chem.* **1988**, *27*, 4587.
- (16) Fussa-Rydel, O.; Zhang, H.-T.; Hupp, J. T.; Leidner, C. R. *Inorg. Chem.* **1989**, *28*, 1533.
- (17) Potts, K. T.; Usifer, D.; Guadalupe, A.; Abruña, H. D. *J. Am. Chem. Soc.* **1987**, *109*, 3961.
- (18) Abruña, H. D.; Denisevich, P.; Umana, M.; Meyer, T. J.; Murray, R. W. *J. Am. Chem. Soc.* **1981**, *103*, 1.

- (19) Guarr, T. F.; Anson, F. C. *J. Phys. Chem.* **1987**, *91*, 4037.

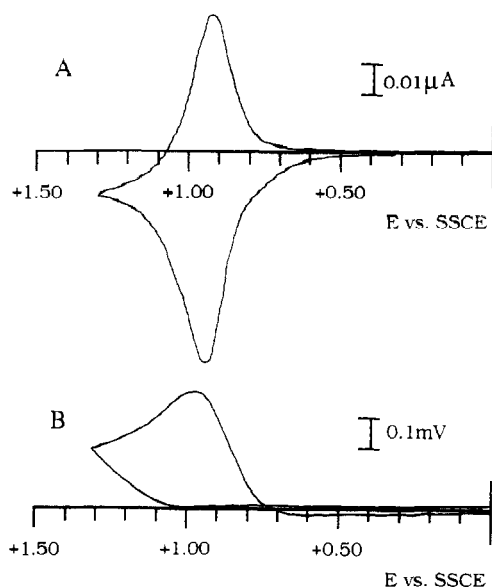


**Figure 2.** Cyclic voltammogram (A) for an electrode array modified with a polymeric film of  $[\text{Fe}(\text{v-bpy})_3]^{2+}$  at 5 mV/s in  $\text{CH}_3\text{CN}/0.1 \text{ M TBAP}$  with the simultaneous measurement of the conductance (B).

sured across the 50-M $\Omega$  load resistor was dependent on the applied bias potential, thus enabling a current-voltage plot to be generated to quantify the film's conductance.

The base-line conductivity of the M(II) species prior to oxidation or reduction was very small (virtually nonconducting), since a polymer film in a single valence state has no states for electron transport. Thus, we will regard the changes in conductance upon generating a mixed-valence state as absolute conductances.

**1. Polymer Film Oxidations.** For the case of polymer film oxidation involving the metal-centered oxidation from the 2+ to the 3+ state, the contribution to the measured voltage drop across the outer two electrodes due to the applied  $E_{\text{bias}}$  was undetectably small due to the very small conductances. The voltage drops across the outer electrodes, however, could be measured precisely and compared qualitatively on a relative scale.

The conductance across the two outer noncontiguous electrodes was measured while the potential applied to the center electrode was varied, thus changing the oxidation state of the polymer film. Both the current and conductance were recorded simultaneously as a function of the applied potential, as is shown in Figure 2 for  $[\text{Fe}(\text{v-bpy})_3]^{2+}$ .

As would be anticipated, the conductance of these electroactive polymers is dependent on the oxidation state of the metal centers within the polymer film with maximal values obtained in the vicinity of the formal potential for the redox process involved where the redox levels would be half-filled. At this point, the concentration gradients from both electrodes meet with the highest slope,<sup>20-22</sup> resulting in the highest conductances. This potential dependent conductance was consistently observed in all polymers employed in this study. However, the magnitude of the conductance was strongly dependent upon the nature of both the metal center and the auxiliary ligands.

Values for the coverage-normalized conductances for the metal-centered oxidations are presented in Table I. For the tris(vinylbipyridine) complexes, values of the coverage-normalized conductances for the M(II/III) couples follow the trend  $\text{Co} < \text{Fe} < \text{Ru} < \text{Os}$ , which correlates very well with the atomic radius of the metal d orbitals,<sup>23</sup> as shown in Figure 3. The larger radial extension of the d orbitals would result in greater orbital overlap enhancing the conductance response.  $[\text{Co}(\text{v-terpy})_2]^{2+}$  was investigated as an analogue for  $[\text{Co}(\text{v-bpy})_3]^{2+}$  because of the low

**Table I.** Coverage-Normalized Conductances for the Mixed-Valent Oxidized Form of Polymers of Transition-Metal Complexes

complex	$g/\Gamma^a$	redox process
$[\text{Os}(\text{v-bpy})_3]^{2+}$	$1.05 \times 10^8$	III/II
$[\text{Ru}(\text{v-bpy})_3]^{2+}$	$6.95 \times 10^7$	III/II
$[\text{Fe}(\text{v-bpy})_3]^{2+}$	$3.47 \times 10^5$	III/II
$[\text{Co}(\text{v-terpy})_2]^{2+}$	$< 10^5$	III/II
$[\text{Co}(\text{v-terpy})_2]^{2+}$	$9.27 \times 10^6$	II/I
$[\text{Fe}(\text{v-bpy})_2(\text{CN})_2]$	$1.45 \times 10^8$	III/II
$[\text{Os}(\text{v-bpy})_2(\text{phen-dione})]^{2+}$	$2.81 \times 10^8$	III/II
$[\text{Os}(\text{v-bpy})_2(5\text{-NH}_2\text{-phen})]^{2+}$	$1.59 \times 10^6$	III/II
$[\text{Os}(5\text{-Cl-phen})_3]^{2+}$	$2.79 \times 10^8$	III/II

<sup>a</sup> Conductance expressed as a voltage drop (mV) divided by surface coverage ( $\text{mol}/\text{cm}^2$ ).

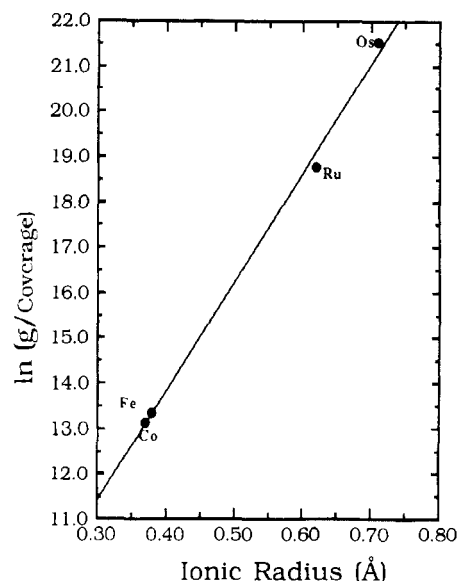


**Figure 3.** Plot of the log of coverage-normalized conductance for the M(III/II) redox process measured across the electrode array versus the atomic radius of the d orbitals for the metal center for  $[\text{M}(\text{v-bpy})_3]$  complexes.

polymerizability of  $[\text{Co}(\text{v-bpy})_3]^{2+}$  due to its chemical instability (ligand loss) in the reduced state necessary for electropolymerization.<sup>24</sup>

Interesting changes in conductance occur upon changing the coordination sphere of a complex or upon looking at a different redox process within a complex. For example, when one of the v-bpy ligands in  $[\text{Fe}(\text{v-bpy})_3]^{2+}$  complex is exchanged for two cyano ligands to yield  $[\text{Fe}(\text{v-bpy})_2(\text{CN})_2]$ , the conductance increases by over 2 orders of magnitude. In an analogous fashion, changing a v-bpy ligand in  $[\text{Os}(\text{v-bpy})_3]^{2+}$  for a phen-dione results in a 3-fold increase in the conductance. In both of these cases we ascribe the enhancement in the conductance to the higher  $\pi$  acidity of the cyano and phen-dione ligands relative to v-bpy. This results in a higher degree of  $\pi$  back-bonding so that more electron density is located at the low-lying  $\pi^*$  orbitals of the ligand and is removed from the metal center, effectively causing partial oxidation of the metal and enhancing the conductance. Other complexes including  $[\text{Os}(\text{v-bpy})_2(4\text{-Me-phen})]^{2+}$  and  $[\text{Os}(\text{v-bpy})_2(5\text{-NH}_2\text{-phen})]^{2+}$  also exhibit conductances that correlate well with the  $\pi$  acidity of the ligands relative to v-bpy.

Collman et al.<sup>25</sup> observed trends in the conductivity of ligand-bridged metalloporphyrin polymers as a function of the bridging ligand. The conductivity was dependent on the ability of the bridging ligand to mediate electron exchange between M(II/III) sites. The relevant interaction was the mixing of the metal  $d\pi$  with the bridging ligand  $\pi^*$  orbitals. Thus, the observed

(20) Pickup, P. G.; Murray, R. W. *J. Electrochem. Soc.* **1984**, *131*, 833.  
 (21) Hagemester, M. P.; White, H. S. *J. Phys. Chem.* **1987**, *91*, 150.  
 (22) Reilly, C. N. *Rev. Pure Appl. Chem.* **1968**, *18*, 137.  
 (23) Fraga, S.; Karwowski, J.; Powell, H. K. *Handbook of Atomic Data*; Elsevier: Amsterdam, 1976; p 465.

(24) Margel, S.; Smith, W.; Anson, F. C. *J. Electrochem. Soc.* **1978**, *125*, 241.  
 (25) Collman, J. P.; McDevitt, J. T.; Leidner, C. R.; Yee, G. T.; Torrance, J. B.; Little, W. A. *J. Am. Chem. Soc.* **1987**, *109*, 4606.

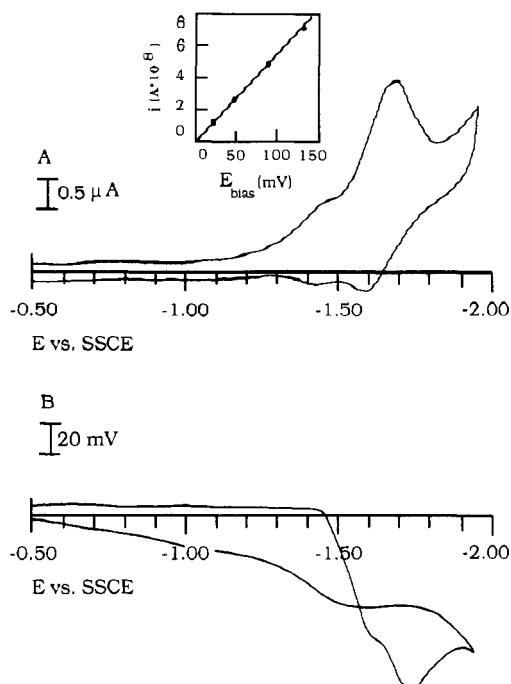


**Figure 4.** Cyclic voltammogram (A) at 5 mV/s for an electrode array modified with a polymeric film of  $[\text{Ru}(\text{v-bpy})_3]^{2+}$  in  $\text{CH}_3\text{CN}/0.1 \text{ M TBAP}$  with the simultaneous measurement of conductance (B). Inset: Plot of the conducting current as a function of the applied bias.

trend was higher conductivities for better  $\pi$ -bonding metals ( $\text{Os} > \text{Ru} \gg \text{Fe}$ ) and for more  $\pi$ -acidic bridging ligands. The increased overlap between the metal ( $d\pi$ ) and the ligand's ( $\pi^*$ ) orbitals that allowed for this increased electron delocalization may also be affecting the redox conduction observed in the  $[\text{M}(\text{v-bpy})_x(\text{L})_y]$  polymers described here.

**2. Polymer Film Reductions.** The data presented thus far were for the  $\text{M}(\text{II}/\text{III})$  couples where electrons from the metal center are predominantly involved, and thus the sensitivity of the conductivity is to the nature of the metal center and its coordination environment. One of the advantages of the complexes employed in this study is that they are stable in multiple oxidation states, which permits the observation of  $2+/1+$  and  $1+/0$  processes where the electron resides primarily on the ligand-based  $\pi^*$  orbitals.

In the case of  $(1+/0)$  reductions, the conductivity of the  $[\text{M}(\text{v-bpy})_3]^{2+}$  ( $\text{M} = \text{Fe}, \text{Ru}, \text{Os}$ ) family is orders of magnitude higher than that for the corresponding  $\text{M}(\text{II}/\text{III})$  processes and, in addition, much smaller differences in conductivity were observed among the various complexes. The smaller differences in conductivity could be accounted for as a perturbation by the metal on the ligand orbitals. This is in marked contrast to the large differences in conductivity observed for the  $\text{M}(\text{II}/\text{III})$  couples. This suggests a significantly different mechanism of charge propagation that could involve closer proximity between the  $\pi$  systems of the ligands or could also be due to a larger electron self-exchange rate constant. Thus, the measured conductivities would be anticipated to be much larger and also not very dependent on the metal center, as was found.

As the polymer films were reduced from the  $2+$  to the  $1+$  and zero charged states, the conductivity was monitored by measuring the current across the load resistor in the external circuit as a function of the changing bias potential. In general, the  $2+/1+$  transition could not be isolated due to the overwhelming change in conductance arising from the  $1+/0$  transition. Murray et al. estimated the conductivity for the  $\text{Os}(\text{II}/\text{I})$  couple to be smaller than that of the  $\text{Os}(\text{I}/0)$  couple by a factor of at least 12.<sup>12</sup> Furthermore, the electrons of the  $\text{Os}(\text{II}/\text{III})$  mixed-valent polymer were found to be 20 times less mobile<sup>10</sup> for a similar complex.

Figure 4 shows the reduction of a  $[\text{Ru}(\text{v-bpy})_3]^{2+}$  polymer film while the external current (proportional to conductivity) is simultaneously measured. The maximum conductance is observed in the mixed-valent state as the polymer is reduced from the  $1+$

**Table II.** Conductivities for the Mixed-Valent ( $1/0$ ) Form of Polymers at Coverages of  $5 \times 10^{-8} \text{ mol/cm}^2$

complex	$10^5 \sigma$ , S/cm	redox process	complex	$10^5 \sigma$ , S/cm	redox process
$[\text{Os}(\text{v-bpy})_3]^{2+}$	3.36	$1/0$	$[\text{Fe}(\text{v-bpy})_3]^{2+}$	1.55	$1/0$
$[\text{Ru}(\text{v-bpy})_3]^{2+}$	2.69	$1/0$			

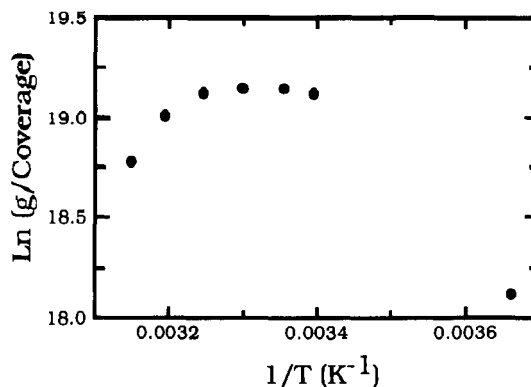


**Figure 5.** Plot of the log of the coverage-normalized conductance versus the reciprocal of temperature for a polymer film of  $[\text{Fe}(\text{v-bpy})_2(\text{CN})_2]^{0/+}$ .

to the zero oxidation state. The actual conductance values were determined by measuring the current for a variety of applied bias potentials to generate a linear  $i$ - $V$  curve from whose slope the film resistance was determined (Figure 4 inset).

After the electrode geometry and film dimensions were accounted for, the conductivity of a film of  $[\text{Ru}(\text{v-bpy})_3]^{1+/0}$  was determined to be  $2.69 \times 10^{-5} \text{ S/cm}$ ; a value comparable to that of poorly doped semiconductors. Conductivities for films of  $[\text{Fe}(\text{v-bpy})_3]^{+/0}$ ,  $[\text{Ru}(\text{v-bpy})_3]^{+/0}$ , and  $[\text{Os}(\text{v-bpy})_3]^{+/0}$  are presented in Table II. The conductivities can be correlated with changes in the radial extension of the  $d$  orbitals of the metal centers as they perturb the ligand orbitals. However, the effect is less dramatic for these conductivity changes than for those observed for the oxidations due to the ligand-localized nature of the reduction.

**3. Mechanisms of Conduction.** Related studies have indicated that the mechanism of electron transport through similar types of redox polymer films is via electron hopping between localized valence states in a mixed-valent film, a process similar to electron self-exchange between redox species in solution.<sup>26</sup>

Consistent with the mechanism of electron hopping are the enhanced conductivities for the mixed-valent states of the complexes, which provide the maximum concentration gradients for electron mobility. A mechanism which involves electrons that are remote to the metal center and in addition are part of an extensively conjugated, largely ligand localized,  $\pi$  network would be consistent with the observed conductivities for the reduced forms of the complexes. On the other hand, a mechanism involving largely metal-centered electrons would be more consistent with the conductivities measured for the metal-based oxidations. Thus, the two mechanisms of charge propagation through these polymer films that we have identified depend on either metal- or ligand-localized orbitals.

We have also investigated the temperature dependence of the conductivity. A reversible and logarithmic dependence of the conductivity with the inverse of temperature (i.e. Arrhenius behavior) was found for all complexes except  $[\text{Fe}(\text{v-bpy})_2(\text{CN})_2]$ . The conductance of the  $[\text{Fe}(\text{v-bpy})_2(\text{CN})_2]$  polymer (Figure 5) exhibited little temperature dependence characteristic of electron mobility through a delocalized band though this response may not necessarily implicate electronic conductivity. This difference in behavior may be due to the fact that, in this particular case, the individual metal complexes are initially uncharged (when iron is in the  $2+$  oxidation state) and upon oxidation acquire a  $+1$  net charge (the iron is present in the  $3+$  oxidation state). Thus,

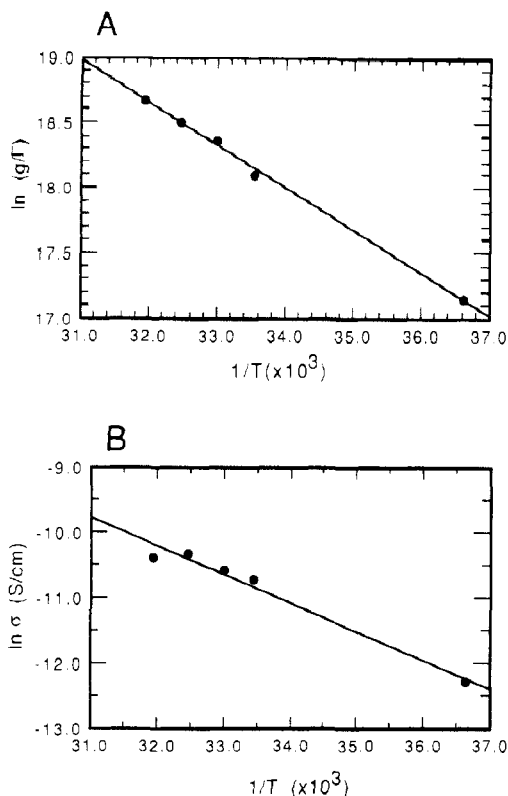


**Figure 6.** Plots of the temperature dependence for (A) the log of coverage-normalized conductance of an electrode array modified with a polymeric film of  $[\text{Os}(\text{v-bpy})_3]^{2+/3+}$  and (B) same as (A) except with  $[\text{Ru}(\text{v-bpy})_3]^{+/0}$ .

substantially different solvation and counterion transport effects may be present in this system relative to the other ones that involve a change from 2+ to 3+ net charge. This type of effect is very well documented in the modified electrode literature, where most significant deviations in voltammetric wave shapes are encountered for systems where one of the redox partners is electrically neutral (e.g. ferrocene).<sup>27</sup>

In general, the temperature response for these polymers indicates an activated process for both the metal-localized oxidations and the ligand-localized reductions (Figure 6), indicating electron or ion movement between localized states rather than electronic conductivity through a delocalized band structure.

The barrier to electron hopping between monomeric units of the metallopolymer is generally recognized to include three components: the motions of the counterions, the polymer lattice fluidity, and the intrinsic energy barrier.<sup>28</sup> For the case of polymerized complexes using the same coupling reaction and the same solvent and counterions in the external solution, no differences between counterion motion and polymer lattice fluidity should exist. Thus, evidence strongly suggests that the differences in the measured conductances are due to changes in the intrinsic energy barrier separating the valence-localized sites for the electron. These variations in the energy barrier have been investigated by determining the activation energy for electron hopping from studies of the temperature dependence of the conductance. A typical value for the activation energy for the  $[\text{Ru}(\text{v-bpy})_3]^{+/0}$  couple is 7.6 kcal/mol, a value similar to those determined for electron self-exchange in solution.

Since for outer-sphere electron-transfer processes the contributions from solvent reorganization dominate the activation energy term, which in turn dictates the rate of electron exchange in solution, the effect of solvent properties may also be very significant in swollen polymer films.

**Table III.** Solvent Dependence for the Conductance of the  $[\text{Os}(\text{v-bpy})_3]^{2+/3+}$  Mixed-Valent Polymer

solvent	$1/\epsilon_{\text{op}} - 1/\epsilon$	$g/\Gamma^a$	solvent	$1/\epsilon_{\text{op}} - 1/\epsilon$	$g/\Gamma^a$
$\text{CH}_3\text{CN}$	0.526	1	$\text{DMF}$	0.462	0.25
$\text{CH}_2\text{Cl}_2$	0.383	0.51	$\text{DMSO}$	0.438	

<sup>a</sup> Conductance values are normalized with respect to coverage and then normalized to one.

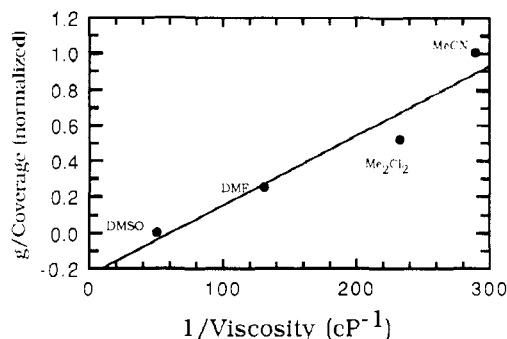


**Figure 7.** Plot of the viscosity dependence, determined by the nature of the solvent, for the normalized conductance for a polymer film of  $[\text{Os}(\text{v-bpy})_3]^{2+/3+}$ .

Since the electron conduction involves the movement of charge, conductivity might be expected to depend on the dielectric properties of the solvent, the appropriate factor from the Marcus theory being  $1/\epsilon_{\text{op}} - 1/\epsilon$ .<sup>30</sup> The correlation between the dielectric constant term and the conductance, as shown in Table III, was not consistent for all the solvents. For instance, the conductance in methylene chloride was twice as large as that in DMF, while the Marcus theory would suggest that, on the basis of dielectric constants, the conductance measured in DMF should be larger. Thus, other factors may be involved that enhance the effectiveness of methylene chloride as a solvent for electron transport. Properties such as the swelling ability of the solvent, which depend on such characteristics as the size of the solvent sphere, may contribute to a higher conductance than would be predicted by dielectric effects alone.

Figure 7 illustrates the correlation between the solvent viscosities and the resulting conductances for  $[\text{Os}(\text{v-bpy})_3]^{3+/2+}$ . The solvent viscosity would affect the conductivity if the mechanism of conduction were dependent upon the movement of ions with their solvation spheres intact or if the viscosity affected the dielectric properties by altering the relaxation times of the solvent.<sup>29</sup> However, when the viscosity of acetonitrile was varied through the same range of values by the addition of poly(vinyl acetate) (which should not alter the properties of the electrode surface or the dielectric constant), the conductance was not dependent upon viscosity. The viscosity was varied from 0.359 to 0.898 cP, a range that covers the viscosities of  $\text{CH}_3\text{CN}$ ,  $\text{CH}_2\text{Cl}_2$ , and  $\text{DMF}$ , but the conductance remained essentially constant at a value near  $6.1 \times 10^7$  mV cm<sup>2</sup>/mol.

However, by introducing a new component (PVA) to the system, other changes beyond variations in the solvent viscosity may also have occurred. For example, if PVA could adsorb on the polymer film, a membrane effect might create local changes in the viscosity of the polymer film. In addition, it is quite possible that the PVA cannot partition into the polymer and thus could not change the polymer film's internal viscosity. In this case, the solvent viscosity within the polymer film may differ from that in the bulk solution. Thus, the variations in conductance may involve a combination of solvent properties including dielectric constant, viscosity, and molecular size.

The relationship between the conductances and the Marcus theory, which predicts a strong correlation between the electron hopping rates and the solvation characteristics, further supports the theory of electron hopping between localized valence states

(27) Peerce, P. J.; Bard, A. J. *J. Electroanal. Chem.* **1980**, *114*, 89.

(28) White, B. A.; Murray, R. W. *J. Am. Chem. Soc.* **1987**, *109*, 2576.

(29) (a) Calef, D. F.; Wolynes, P. G. *J. Phys. Chem.* **1983**, *87*, 3387. (b) Calef, D. F.; Wolynes, P. G. *J. Phys. Chem.* **1983**, *87*, 470.

(30) (a) Marcus, R. A. *J. Chem. Phys.* **1965**, *43*, 679. (b) Marcus, R. A. *Annu. Rev. Phys. Chem.* **1964**, *15*, 155.

**Table IV.** Electrolyte Dependence of the Coverage-Normalized Conductance of Mixed-Valent (III/II) Polymers

complex	electrolyte	anion diameter, Å	$g/\Gamma$
$[\text{Os}(\text{v-bpy})_3]^{2+}$	TBAP	3.70	$3.81 \times 10^7$
$[\text{Os}(\text{v-bpy})_3]^{2+}$	(TBA)BF <sub>4</sub>	4.35	$2.59 \times 10^7$
$[\text{Os}(\text{v-bpy})_3]^{2+}$	(TBA)PF <sub>6</sub>	3.34	$2.63 \times 10^7$
$[\text{Fe}(\text{v-bpy})_2(\text{CN})_2]$	TBAP	3.70	$2.80 \times 10^8$
$[\text{Fe}(\text{v-bpy})_2(\text{CN})_2]$	(TMA)Ts	7.98	$3.18 \times 10^8$

to explain conductances in these polymers.

Consistent with this theory is the observation that the conductance observed for the Co(II/I) couple is several orders of magnitude higher than that for the Co(II/III) couple for polymerized films of  $[\text{Co}(\text{v-terpy})_2]^{2+}$ . These values follow the same trend as the apparent diffusion coefficients measured by chronoamperometry.<sup>31</sup> Also, the conductance for the  $[\text{Os}(\text{5-Cl-phen})_3]^{2+/3+}$  mixed-valent polymer film is higher than that observed for the  $[\text{Os}(\text{v-bpy})_3]^{2+/3+}$  film, while the coordination environments are very similar except for the much shorter electron-hopping distance for the  $[\text{Os}(\text{5-Cl-phen})_3]^{2+/3+}$  polymer film due to its polymerization mechanism. The intrinsic energy barrier to hopping is thus reduced for smaller hopping distances, leading to increased electron mobility.

One further possible explanation for the observed behavior of these polymer films is that mobile counterions (rather than electrons) from the external solution maintain the charge mobility. This mechanism is often referred to as a type of ionic conduction. A variety of different-sized anions with the same charge were used in the supporting electrolyte, since if ions were responsible for the conduction, the size of the ion would affect its magnitude. The use of the smallest anions (with their accompanying solvation

spheres) should result in the largest conductances. However, as shown in Table IV, the size of the anion had relatively little effect on the conductances. In acetonitrile, with 0.1 M supporting electrolyte, the use of various anions whose diameters ranged from 3.34 to 4.35 Å did not cause a significant difference in the normalized conductances for the  $[\text{Os}(\text{v-bpy})_3]^{2+/3+}$  polymer film. Similarly, in DMF, even the very large toluenesulfonate anion did not reduce the conductance for the  $[\text{Fe}(\text{v-bpy})_2(\text{CN})_2]^{0/+}$  polymer film. The tetraphenylborate anion would have been an interesting comparison due to its very large diameter; however, the anion oxidizes at potentials lower than those of the metal centers of interest. The independence of the conductance on the identity of the counteranion provides further evidence for charge transport via electrons. Furthermore, the large difference in redox conduction between the II/III and the I/0 mixed-valent states are difficult to reconcile if counterion mobility is limiting rather than electron transport, since the counterion diffusion rate would have to be significantly altered by a change in the polymer oxidation state.

The trends presented here demonstrate the influence of the atomic radius of the metal centers and the  $\pi$ -back-bonding ability of the ligands on conductance. This suggests that lowering the activation barrier between localized states (in this case each transition-metal complex) produces an increase in the conductance. Investigation of the appropriate copolymers may provide further insight into limiting factors in conduction.

**Acknowledgment.** Financial support by the Materials Science Center at Cornell University is gratefully acknowledged. H.C.H. acknowledges support by a fellowship from the Aerospace Corp. H.D.A. is a recipient of a Presidential Young Investigator Award (1984-1989) and a Sloan Fellowship (1987-1991).

**Registry No.**  $[\text{Os}(\text{v-bpy})_3]^{2+}$ , 97056-94-5;  $[\text{Ru}(\text{v-bpy})_3]^{2+}$ , 81315-14-2;  $[\text{Fe}(\text{v-phy})_3]^{2+}$ , 81315-15-3;  $[\text{Co}(\text{v-terpy})_2]^{2+}$ , 108270-57-1;  $[\text{Fe}(\text{v-bpy})_2(\text{CN})_2]$ , 119058-92-3;  $[\text{Os}(\text{v-bpy})_2(\text{phen-dione})]^{2+}$ , 124355-17-5;  $[\text{Os}(\text{v-bpy})_2(\text{5-NH}_2\text{-phen})]^{2+}$ , 124355-19-7;  $[\text{Os}(\text{5-Cl-phen})_3]^{2+}$ , 124355-20-0.

(31) Guadalupe, A. R.; Usifer, D. A.; Potts, K. T.; Hurrell, H. C.; Mogstad, A.-L.; Abruña, H. D. *J. Am. Chem. Soc.* **1988**, *110*, 3462.

Contribution from the Departments of Chemistry, Louisiana State University, Baton Rouge, Louisiana 70803, and University of Louisville, Louisville, Kentucky 40506, and Control Research and Development, Upjohn Pharmaceuticals Limited, Tsukuba 300-42, Japan

## Rotation of the Cyclopentadienyl Ligand in Bis( $\mu$ -carbonyl)bis(carbonylcyclopentadienyliron)(*Fe-Fe*) in the Solid State As Determined from Solid-State Deuterium NMR Spectroscopy

Maria I. Altbach,<sup>1a</sup> Yukio Hiyama,<sup>\*1b</sup> Richard J. Wittebort,<sup>\*1c</sup> and Leslie G. Butler<sup>\*1d</sup>

Received January 9, 1989

The motion of the cyclopentadienyl ring in  $(\mu\text{-CO})_2[\text{FeCp}^d(\text{CO})]_2$  ( $\text{Cp}^d = \text{ca. } 70\% \text{ deuteriated } \eta^5\text{-cyclopentadienyl}$ ) in the solid state has been studied from 100 to 300 K by solid-state deuterium NMR methods. The deuterium spin-lattice relaxation times show that the orientation of the cyclopentadienyl ligands, Cp, is averaged among the five sites of the ring with nearest-neighbor jump rates in the range  $1.20 (24) \times 10^7$  to  $2.4 (5) \times 10^{11} \text{ s}^{-1}$ . The activation energy for the process is 12.5 (3) kJ/mol. The kinetic parameters obtained in this work are similar to the values for the reorientation of the cyclopentadienyl ligands in other organometallic compounds as determined with different techniques. The results of this work show that solid-state deuterium NMR spectroscopy uniquely complements existing techniques for the study of the motional properties in organometallic systems.

### Introduction

In the last decade, deuterium NMR spectroscopy has become a very popular technique for the study of dynamic processes in the solid state.<sup>2</sup> This technique makes possible the investigation of different motional modes over a wide range of rates. Dynamic processes occurring with rates in the range  $10^4$ - $10^8 \text{ s}^{-1}$  can be investigated by a line-shape analysis of the deuterium NMR spectrum of a powder. For motions on the order of and faster than  $10^8 \text{ s}^{-1}$ , the line shapes become independent of the exchange

rate; an analysis of the partially relaxed spectra obtained from deuterium spin-lattice relaxation time ( $T_1$ ) experiments is used to discriminate among the types and rates of motion. With the availability of computer programs capable of simulating both the

- (1) (a) Present address: Department of Chemistry, University of Arizona, Tucson, AZ 85721. (b) Present address: Upjohn Pharmaceutical Limited, 17th Floor, Green Tower Building 6-14-1, Nishi Shinjuku, Tokyo 160, Japan. (c) University of Louisville. (d) Louisiana State University.  
(2) (a) Jelinski, L. W. *Annu. Rev. Matter. Sci.* **1985**, *15*, 359-77. (b) Torchia, D. A. *Annu. Rev. Biophys. Bioeng.* **1984**, *13*, 125-44. (c) Spiess, H. W. *Adv. Polym. Sci.* **1985**, *66*, 23-58.

\* To whom correspondence should be addressed.